Electronic Supplementary Information

Rational Design of SnO_2@C Nanocomposties for Lithium Ion Batteries by Utilizing Adsorption Properties of MOFs

Meihui Wang,† Hao Yang,† Xianlong Zhou, Wei Shi,* Zhen Zhou* and Peng Cheng

Nankai University, Tianjin 300071, PR China. E-mail: shiwei@nankai.edu.cn (WS);

zhouzhen@nankai.edu.cn (ZZ).

*To whom correspondence should be addressed

Experimental Section

Synthesis

Preparation of HKUST-1

The reagents were used as obtained from commercial sources of analytical grade without further purification. HKUST-1 was prepared follow the typical reported methods.[1] 4.375g $Cu(NO_3)_2 \cdot 3H_2O$ (18mmol) was dissolved in 60mL of deionized water, while 2.10g trimesic acid (10mmol) was dissolved in 60mL of ethanol. Mix up the two solutions, and then divide equally into six Teflon kettle (each with 25mL volume). Keep in 120℃ for 12 hours. Filtering to get crystal, and washing twice with hot ethanol before drying in an oven at 100℃.

Preparation of H600 and H600-HNO_3

The blue dry HKUST-1 crystal was homogeneously dispersed in a ceramic boat before placing the ceramic into the furnace. After the sample was exposed to a flow of argon (500mL/min) at room temperature for 40 min. The furnace was heated to the targeted carbonizing temperature using a heating rate of 5℃/min. At 600℃ to get H600. The different carbonizations were soaking and washing by *wt.*50% nitric acid to get H600-HNO_3. Washing H600, H600-HNO_3 with deionized water five times and drying at 100℃ in an oven.

Preparation of Sn-Cu@C & SnO_2@C

Dry the blue HKUST-1 crystal inside a glass flask at 140℃ in a vacuum oven for 8 hours. Seal up with a rubber plug as soon as the flask was taken out. 1mol/L stannous chloride solution was added to the dry powders by a syringe. And the

amount of the solution was limited by just wetting the powders. Dry the sample again in a vacuum oven at 100℃. Carbonizing at 600℃ as preparation of the H600 after grinding the sample to homogeneous powders, which resulted in Sn-Cu@C. The Sn-Cu@C were soaking and washing by *wt.*50% nitric acid to get SnO_2@C. We also tried heating during washing gingerly in a water bath at 40 degree centigrade to remove the little amount of $Cu_{10}Sn_3$, but it suddenly bubbled a lot and all the black solid disappeared in ten minutes. This result indicates that the excess HNO_3 with heating is able to remove $Cu_{10}Sn_3$ completely but also destroy the whole structure.

Characterization

The Brunner-Emmet-Teller (BET) specific surface area and porosity (based on Barrett-Joyner-Halenda method) were determined by N_2 adsorption/desorption isotherms through Micromeritics ASAP 2020 system. Further structures were analyzed Thermogravimetric Analysis (TGA, Rigaku PTC-10A TG-DTA instrument, heat rate of 10 °C/min). Inductive Coupled Plasma Atomic Emission Spectrometer (ICP-AES) was tested by PerkinElmer Optima 8300 inductively coupled plasma emission spectrometer. Elemental analysis was analyzed by Vario EL CUBE. Then the samples were characterized by X-ray photoelectron spectroscopy (XPS) on an ULVAC-PHI by using PHI 5000 Versa Probe system. And X-ray diffraction was performed on a Rigaku MiniFlex II diffractometer with Cu Kα radiation (λ=1.5418 Å). Morphology and texture observations were operated on Nova NanoSEM 430 and JEOL JSM-7500F instrument. Transmission electron microscope (TEM) and high resolution transmission electron microscope (HRTEM) were measured by FEI Tecnai

G2F-20 microscope. The cross sections were quenched in liquid nitrogen at 77 K before the electrodes were truncated.

Electrochemical measurements

In a typical electrode preparation, active materials, conductive carbon black (Super P) and poly(vinylidene fluoride) (PVDF) were mixed with a ratio of 75:15:10 to form a slurry. The thick mixture was doctor bladed onto Cu foil and dried at 80℃, 110℃ for 2h and 10h respectively in vacuum. Electrochemical performances were evaluated in CR2025-type coin cells assembled in a high-purity argon-filled glove box. Lithium metal served as counter and reference electrodes. The electrolyte was comprised of a solution made by 1 M LiPF6 in dimethyl carbonate (DMC)/ethyl methyl carbonate (EMC)/ethylene carbonate (EC) mixture (1:1:1 v/v/v) while Celgard 2400 membrane was used as a separator. The galvanostatic cycling performances were evaluated on LAND-CT2001A battery testers. CV was performed on CHI600C electrochemical workstation at scan rate of 0.1 mV/s. All the above measurements were conducted at room temperature.

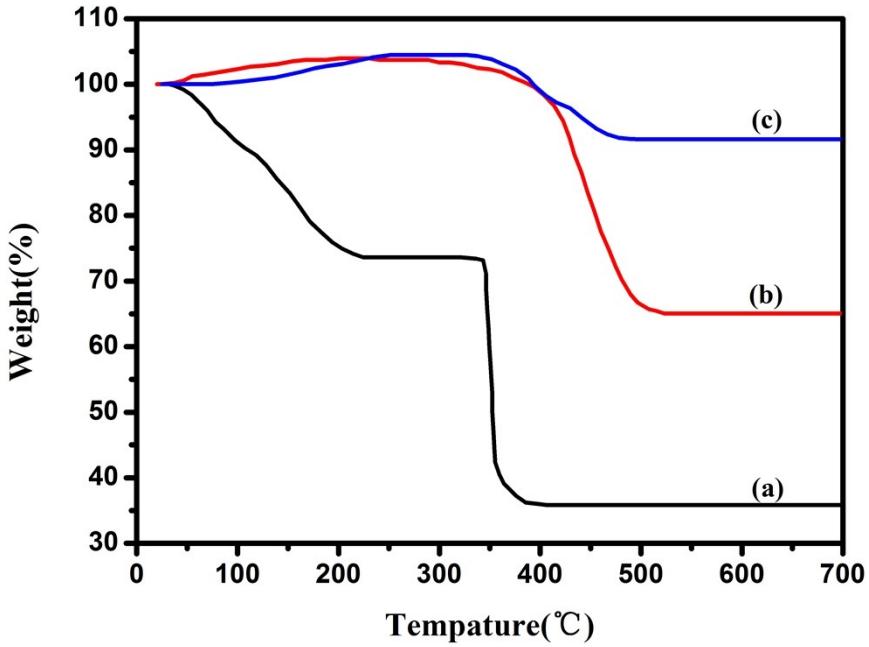

Fig. S1 TGA curve of the HKUST-1(a), SnO_2@C(b), Sn-Cu@C(c) composites in air at a heating rate of 10 ºC min^{-1}. The weight loss for the composite is 34.8%, which result from both the decomposition of carbon structure and the oxidation of Sn to SnO_2. It can be observed that the curves b and c increase between 100 ºC to 300 ºC, which is attributed to the oxidation of Sn and Cu. Because of the existence of Cu, the remains of Sn-Cu@C is higher than that of SnO_2@C.

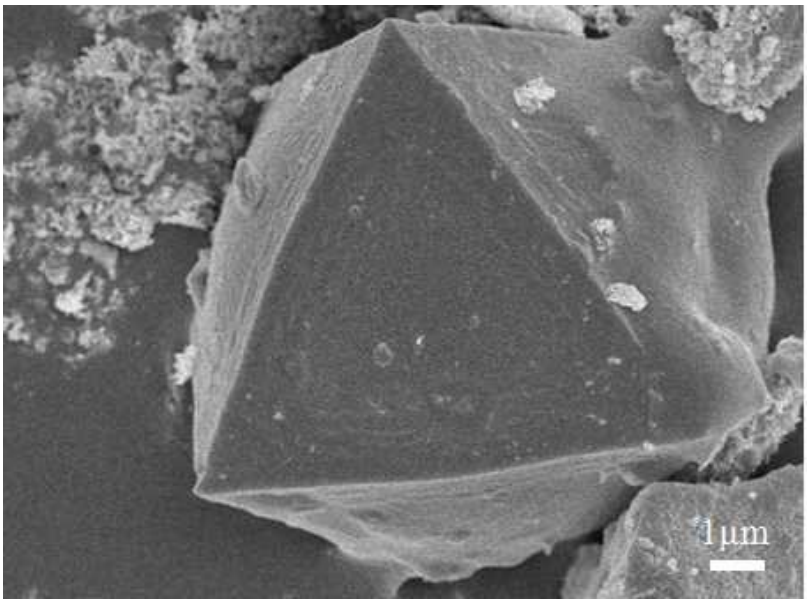

Fig. S2 SEM image of H600-HNO_3. It is clear that H600-HNO_3 composite holds the octahedral shape, indicating that the remove of Cu by HNO_3 will not destroy the morphology of the composite.

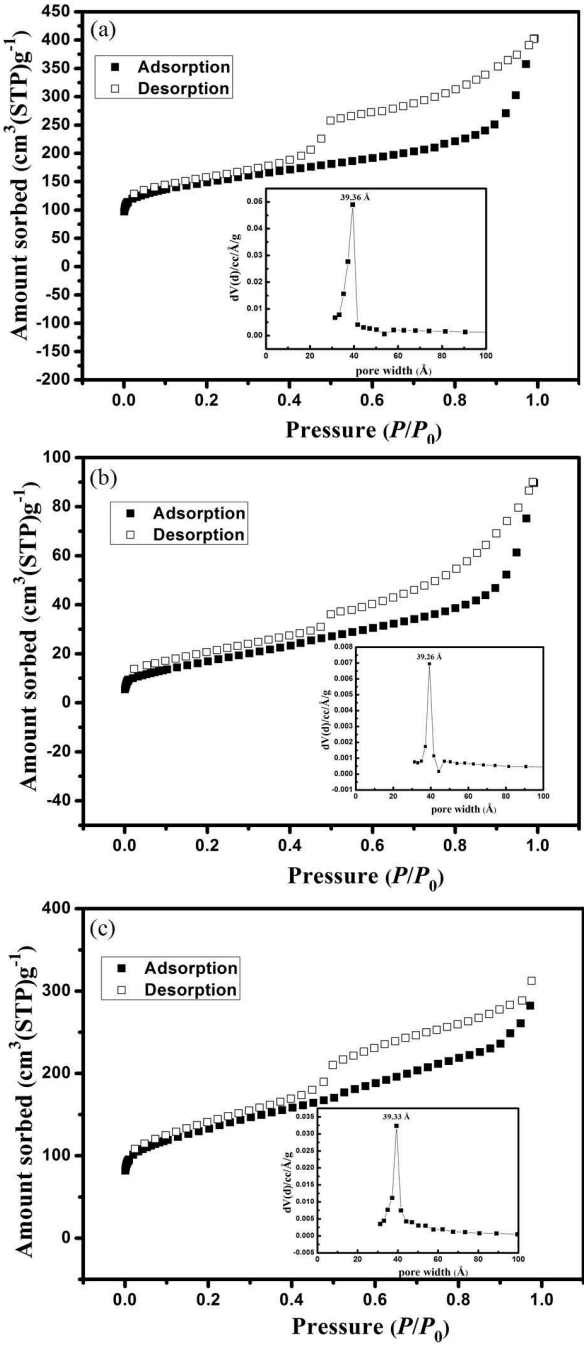

Fig. S3 Nitrogen isotherms at 77 K and pore size distribution curve (inset) of H600-HNO_3 (a), Sn-Cu@C (b) and SnO_2@C (c). The BET specific surface area of H600-HNO_3 (a), Sn-Cu@C (b) and SnO_2@C is 540.228 m^2 g^{-1}, 64.027 m^2 g^{-1} and 474.158 m^2 g^{-1}.There are no distinct difference between the pore diameters of these three composites but the surface areas, which implies the stability of the carbon structure even after the doping of Sn and the disposal of HNO_3 solution. And such great increase from Sn-Cu@C to SnO_2@C indicates that the dissolution of Cu contributes to the large vacant space, which is beneficial for remitting the volume expansion of SnO_2.

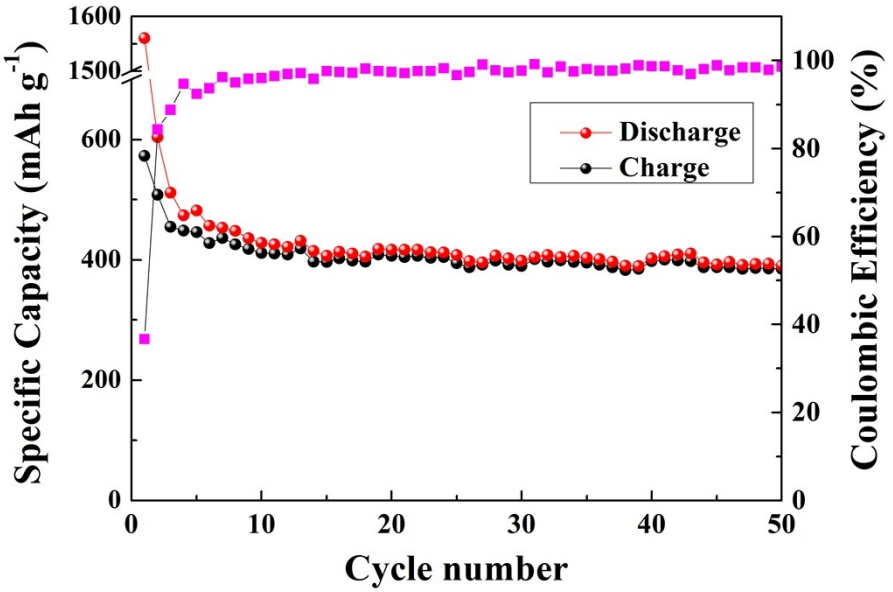

Fig. S4 Cycling performance of H600-HNO_3 at a current density of 100 mA g^{-1}.

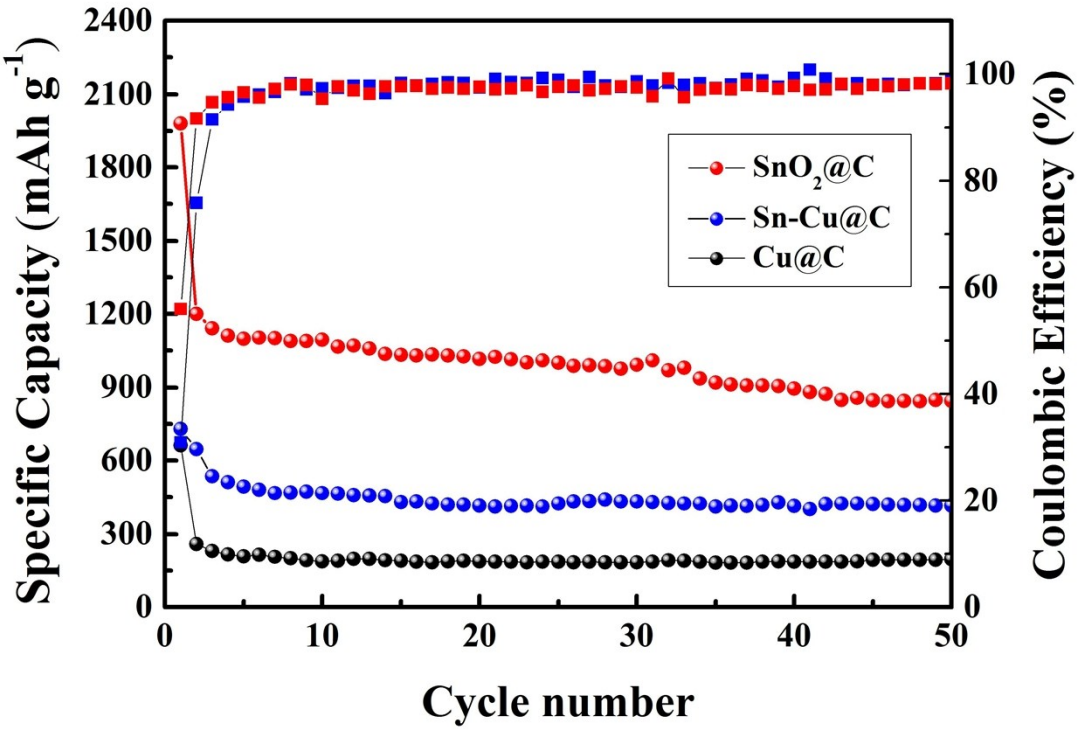

Fig. S5 Cycling performance of SnO_2@C,Sn-Cu@C,Cu@C at a current density of 100 mA g^{-1}.

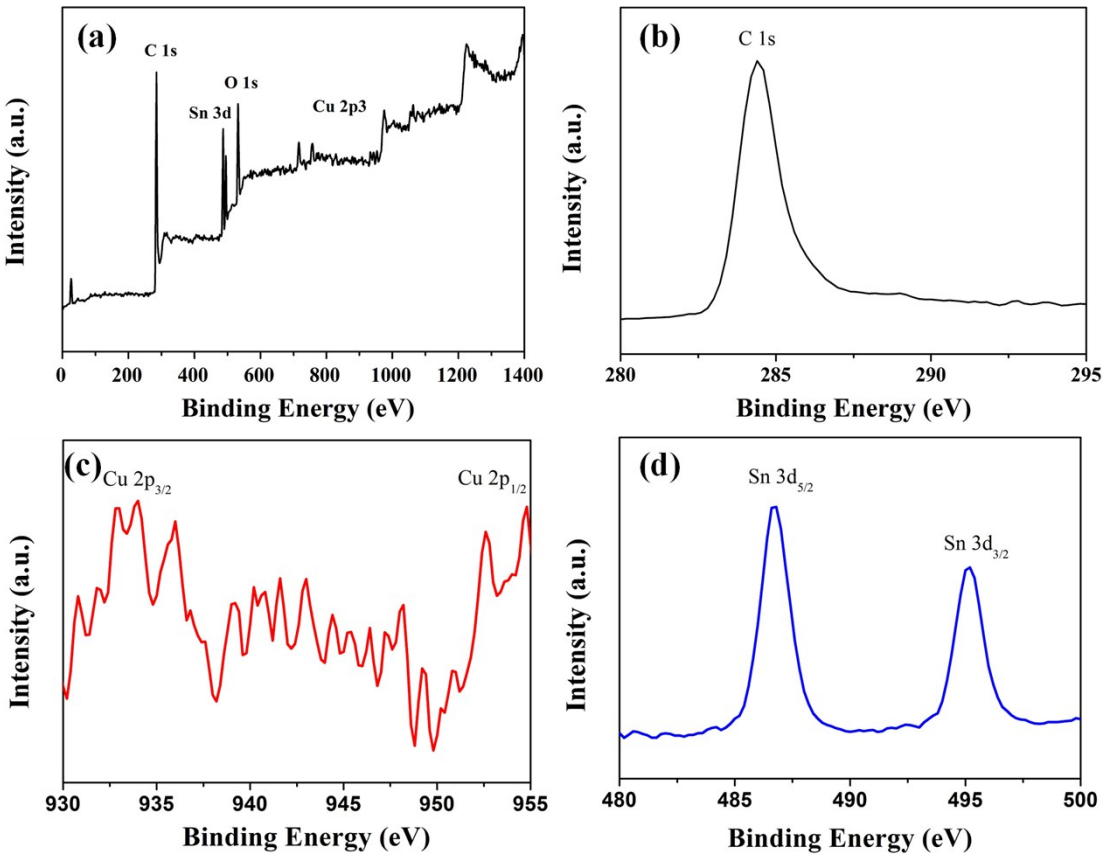

Fig. S6 XPS spectra of a) SnO_2@C, b) C 1s narrow scan of SnO_2@C, c) Cu 2p3 narrow scan of SnO_2@C, d)Sn 3d narrow scan of SnO_2@C. The binding energy of Sn is in tune with SnO_2.

Table. S1 Elemental composition analyzed by different methods (in wt%).

	SnO_2	Cu	C	H
ICP-AES	48.69			
Element Analysis			48.26	1.64
XPS	31.57	1.6	66.83	

Table. S2 Comparison of our sample with previously published SnO_2/C-based anode materials for lithium ion batteries in terms of synthesis route, SnO_2 content and rate capability.

Electrodes	Synthesis route	SnO2 content	Rate Capacity (mAh g^{-1})/ Current density (A g^{-1})/ Cycle Number
SnO_2@C (This work)	**Introduction and Pyrolysis**	**46wt%**	**880/0.1/200**
SnO_2-NG[2]	Solvothermal	75wt%	853/0.78/275
SnO_2/Layed Carbon[3]	Solvothermal	80wt%	700/0.1/115
SnO_2/Titanate[4]	Sol-gel	60wt%	507/0.1/50
SnO_2-GNRs[5]	Ultrasonication	80wt%	825/0.1/50
SnO_2 NPs@Graphene[6]	Template	88wt%	696/0.5/300
Bowl-like SnO_2@Carbon Hollow Particles[7]	Template	76.3wt%	963/0.4/100

REFERENCES

1. S. Bordiga, L. Regli, F. Bonino, E. Groppo, C. Lamberti, B. Xiao, P. S. Wheatley, R. E. Morris and

A. Zecchina, *Phys. Chem. Chem. Phys.*, 2007, **9**, 2676.

2. W. Zhou, J. Wang, F. Zhang, S. Liu, J. Wang, D. Yina and L. Wang., *Chem. Commun.*, 2015, **51**, 3660.

3. J. Kong, W. A. Yee, L. Yang, Y. Wei, S. L. Phua, H. G. Ong, J. M. Ang, X. Li and X. Lu, *Chem. Commun.*, 2012, **48**, 10316.

4. J. H. Kang, S. M. Paek and J. H. Choy, *Chem. Commun.*, 2012, **48**, 458.

5. J. Lin, Z. Peng, C. Xiang, G. Ruan, Z. Yan, D. Natelson and J. M. Tour, *ACS nano*, 2013, **7**, 6001.

6. X. Zhou, Y.-X. Yin, L.-J. Wan and Y.-G. Guo, *J. Mater. Chem.*, 2012, **22**, 17456.

7. J. Liang, X. Y. Yu, H. Zhou, H. B. Wu, S. Ding and X. W. D. Lou, *Angew. Chem. Int. Ed.*, 2015, **53**, 12803.